Comparison of the Structure of Liquid Amides as Determined by Diffraction Experiments and Molecular Dynamics Simulations

Pia C. Schoester[a], Manfred D. Zeidler[a], Tamás Radnai[b], and Philippe A. Bopp[c]

[a] Institut für Physikalische Chemie, Rheinisch-Westfälische Technische Hochschule,
Templergraben 59, D-52062 Aachen.
[b] Central Research Institute for Chemistry, Hungarian Academy of Sciences, P.O. Box 17,
H-1525 Budapest.
[c] Laboratoire de Spectroscopie Moléculaire et Cristalline (CNRS URA 124),
Université Bordeaux I, 351 Cours de la Libération, F-33405 Talence Cedex.

Z. Naturforsch. **50a**, 38–50 (1995); received October 8, 1994

Dedicated to Professor Hitoshi Ohtaki on the occasion of his 60th birthday

The intermolecular structures of liquid formamide, N-methylformamide and N,N-dimethylformamide at room temperature are studied by means of NVE molecular dynamics computer simulations. Newly developed flexible models are used. X-ray and neutron weighted structure and total radial pair distribution functions are computed from the simulated site-site pair distribution functions. They are compared with experimental results. The agreement is usually satisfactory as far as heavy atom pairs are concerned while the lengths of the hydrogen bonds are found to be systematically too long in the simulations.

I. Introduction

Formamide (FA), N-methylformamide (NMF) and N,N-dimethylformamide (DMF) are the simplest amide compounds. These liquids are widely used organic solvents with interesting physicochemical properties. The molecules have high dipole moments and should form well-ordered structures in the liquid phase. Another important feature of this series is that the number of possible hydrogen-bonds decreases from 4 per molecule in FA to zero in DMF. Hydrogen-bonds are formed between the C=O group of one molecule and the N–H groups of its neighbors. Therefore, a comparative study of the structure of these liquids should lead to a better understanding of the role of the O···H–N type H-bonds, the dipole-dipole interactions, and the yan der Waals-type interactions toward the formation of the local order.

The structures of the three liquids have already been studied by several experimental and theoretical methods. The knowledge about the FA seems to be the most extensive. Here we refer to the experimental studies by X-ray diffraction (XD) [1], by a combination of XD, neutron diffraction (ND) and electron diffraction (ED) [2] and by an ND method with several isotopic substitutions [3]. These experiments provided the intermolecular distances of H-bonded molecules in the liquids. The usual interpretation is that the predominant arrangement between neighboring molecules is the linear chain. Computer simulations have also been performed on liquid amide systems. A Monte Carlo (MC) simulation [4] with OPLS potentials and a more recent molecular dynamics (MD) simulation [5], in which the newly developed test-particle model potential was applied, have led to somewhat contradictory results for the partial pair distribution functions. In the latter work the local structure is only in partial agreement with the experiments and with the MC work. The energetically most favorable nearest-neighbor structure was thought to be the cyclic dimer.

As to NMF, we mention here an XD work [6] suggesting a linear chain structure without extended network-formation, and an ND study [7] with two isotopic substitutions, in which the intramolecular conformations rather than the liquid structure were studied. No previous computer simulations were found in the literature. Recently a systematic investigation of liquid NMF by a combination of several experimental (XD, ND, ED) and computer simulation studies has been completed [8]. Results will be partially reported here.

The structure of liquid DMF is considered to be known. This knowledge is, however, based only on two XD measurements [9, 10], a MC simulation [5] and a MD study [11]. No further studies, e.g. by the ND method, are known. The purpose of the present

---

Reprint requests to Prof. Dr. M. D. Zeidler.

0932-0784 / 95 / 0100-0038 $ 06.00 © – Verlag der Zeitschrift für Naturforschung, D-72027 Tübingen

paper is to provide a systematic study of the three liquids by the MD method. For this purpose we attempt to develop a consistent set of potential functions for the three systems. Here we report the method for the determination of the intra- and intermolecular potentials and a few checks for the accuracy of the parameters. The major part of the paper discusses the structural results obtained from the MD-simulations. The intermolecular pair distribution functions (pdf) and the scattering functions constructed from them are systematically compared with those from previous experimental and simulation studies. The energetic and dynamical properties of the liquids obtained from the present simulations will be reported in a subsequent paper.

II. Details of the Simulations

Flexible models with six sites centered at the positions of the atoms are used; each methyl group is treated as one site. A flexible model allows for the distortion of the molecules due to the interactions with their neighbors. The total interaction potential is assumed to be the sum of the intra- and intermolecular interaction potentials.

The molecular equilibrium geometries are chosen to match experimental data. The values given in Table 1 are critically averaged values from the literature for the formamides [1–3, 6, 9, 10, 12–21]. We assume, as it is usual, that the electrostatic contribution to the intermolecular potential is adequately represented by point charges on the atoms. There are some literature data for the charge distributions of the formamides, but the calculated dipole moments differ from the experimental ones. The polarisability of the molecules is ignored here.

Table 1. Parameters of the intramolecular geometries of the amide molecules. R1 is next to the oxygen. R1 in FA and R2 in FA and NMF are hydrogen. Else they are CH_3.

	FA	NMF	DMF
$r_{\mathrm{NR1}}/\mathrm{Å}$	1.008	1.458	1.460
$r_{\mathrm{NR2}}/\mathrm{Å}$	1.007	1.017	1.460
$r_{\mathrm{CH}}/\mathrm{Å}$	1.098	1.100	1.100
$r_{\mathrm{CO}}/\mathrm{Å}$	1.223	1.220	1.230
$r_{\mathrm{CN}}/\mathrm{Å}$	1.358	1.352	1.355
$\delta_{\mathrm{CNR1}}/\mathrm{deg}$	119	119	118
$\delta_{\mathrm{R1NR2}}/\mathrm{deg}$	120	120	124
$\delta_{\mathrm{R2NC}}/\mathrm{deg}$	121	121	118
$\delta_{\mathrm{NCH}}/\mathrm{deg}$	113	113	114
$\delta_{\mathrm{HCO}}/\mathrm{deg}$	123	123	123
$\delta_{\mathrm{OCN}}/\mathrm{deg}$	124	124	123

A charge distribution for FA is taken from ab initio calculations [3]. This charge distribution reproduces the experimental dipole moment. Since similar calculations are not available for NMF and DMF, CNDO calculations of FA and DMF [22] are used to determine the trends in the charge distributions. The final charge distribution for NMF and DMF are determined by considering these differences and by scaling to the experimental dipole moments. The short-range interactions are described by Lennard-Jones-sites on the atoms, the CH_3-groups are approximated as one site. The homonuclear Lennard-Jones parameters are determined from selected published data [4, 23–29]. The total intermolecular interaction potential is thus the sum of pair potentials V_{ij} acting between the sites i and j on different molecules:

$$V = \sum_{i,j} V_{ij} = \sum_{i,j} \left(\frac{C q_i q_j}{r_{ij}} + 4 \varepsilon_{ij} \left(\left(\frac{\sigma_{ij}}{r_{ij}} \right)^{12} - \left(\frac{\sigma_{ij}}{r_{ij}} \right)^{6} \right) \right), \tag{1}$$

where $C = e^2/(4\pi\varepsilon_0)$, q_i and q_j are fractional charges in units of e, the elementary charge, r_{ij} is the distance between sites i and j, ε and σ are the Lennard-Jones parameters and ε_0 is the vacuum permittivity. The partial charges and the σ- and ε-parameters are listed in Tables 2 and 3 together with the resulting molecular dipole moments for the intramolecular equilibrium geometries. The Lennard-Jones parameters for heteronuclear pair interactions are calculated by Kong's rule [30].

The choice of parameters for the intermolecular potential of DMF is tested on a bimolecular system. Two DMF molecules are fixed at the experimental intramolecular geometry and the intermolecular potential is rotationally optimized on a grid of points. The variables are varied both individually and simultaneously. The arrangement of lowest energy (−24.3 kJ mol^{-1}, "dimerisation energy") is obtained for a sandwich structure with antiparallel dipoles and a distance between the two molecular planes of 3.7 Å. The result that the most stable amide structure is of a sandwich type was also found by Jorgensen and Swenson for DMF [4] and by Radnai et al. for a mixture of acetonitril with DMF [10].

The intramolecular potential is described by a force field up to second order in terms of bond stretches, angle and out-of-plane bends, and torsions, requiring 15 force constants: 6 for the stretches, 5 for the angle bends, 3 for the out-of-plane bends and one for the

Table 2. Values of the partial charges q_i at the i-th site of a molecule, resulting dipole moments μ and angle ϕ between the direction of the dipole moment and the plane of the molecule.

	FA [13]	NMF	DMF
q_{R1}/e	0.300	0.205	0.215
q_{R2}/e	0.280	0.300	0.205
q_H/e	−0.015	−0.018	−0.020
q_O/e	−0.479	−0.490	−0.510
q_N/e	−0.584	−0.510	−0.430
q_C/e	0.498	0.513	0.540
μ/D (calc.)	3.69	3.86	3.82
μ/D (exp.)	3.71 [16]	3.86 [6]	3.80−3.86 [6]
ϕ/deg (calc.)	−36.1	−37.2	−38.3
ϕ/deg (exp.)	−39.6	−39.6	−39.6

Table 3. Lennard-Jones parameters used for the homonuclear pair interaction for amides.

	H−H	C−C	O−O	N−N	Me−Me
σ/Å	2.200	3.375	3.405	3.647	3.807
$\varepsilon/10^{-21}$ J	0.1319	0.7020	1.6367	1.3227	1.2771

torsion. In order to determine them, several intramolecular potentials are taken from the literature [31−37] and tested by constructing the Wilson GF-matrix and comparing the calculated frequencies with experimental data [38−45]. The best agreement is obtained with a potential for DMF generated by Schmid and Brodbek [37] in which a few of the original parameters are additionally adjusted. The force constants for FA and NMF are adjusted by using the results of semiempirical calculations. A detailed description of the parameters is omitted here; the calculated frequencies are compared with the experimental ones in Table 4.

The simulations are carried out in the NVE ensemble. The dimensions of the cubic boxes are determined from the experimental densities at 298 K (FA: 1.1292 g/cm^3, NMF: 0.9988 g/cm^3, DMF: 0.9439 g/cm^3). The boxlengths are 25.68 Å for FA, 29.18 Å for NMF and 32.05 Å for DMF. The average temperature of the simulations is 296 K−298 K. The number of molecules in the box, 256, corresponds to 1536 sites. The Ewald method [46] is used for the calculation of the Coulomb forces and energies while the shifted force potential method [47] is employed for the non-Coulombic parts of the potentials. The cut-off radius is set to half the boxlength.

Table 4. Comparison of the calculated and experimental [38−45] vibrational frequencies for the three amide molecules.

FA [$\tilde{\nu}$/cm^{-1}]		NMF [$\tilde{\nu}$/cm^{-1}]		DMF [$\tilde{\nu}$/cm^{-1}]	
exp.	calc.	exp.	calc.	exp.	calc.
3330−3570	3490	3301−3480	3305	2870−2860	2858
3190−3451	3373	2732−2877	2870	1684−1714	1711
2852−2896	2886	1667−1724	1836	1495−1512	1513
1690−1740	1718	1498−1546	1588	1381−1410	1373
1572−1608	1610	1386−1387	1335	1250−1268	1210
1378−1393	1400	1200−1248	1123	1064−1095	1072
1253−1315	1257	948− 960	970	865− 870	868
1086−1095	1101	750− 778	763	660− 662	616
1030−1056	1030	676− 720	675	400− 405	410
602− 750	726	618− 624	781	360	357
564− 608	611	353− 356	275	320	315
200− 289	190	297− 302	78	65	62

The systems are equilibrated for about 10 000 timesteps of $2 \cdot 10^{-16}$ s each, at every 100th timestep the temperature is rescaled to 298 K. Then data collection is started for a total number of timesteps of 51 250 for FA, 54 000 for NMF and 62 250 for DMF. Further details and results of the MD simulations will be published elsewhere.

III. Diffraction Experiments

Since the diffraction experiments were carried out and analyzed at different laboratories and with different methods, it is difficult to compare them directly with each other and with the simulation results. The experimental data are thus first transformed to a common form. This procedure involves assumptions on the type of scattering unit and on the forms of the self scattering terms, and renormalization. This treatment can slightly modify the shapes of the structure functions, but it has only little influence on the physical interpretation of the results.

Measured scattering data can furthermore not be translated directly into structure functions. Various corrections have to be performed, e.g. for the background, absorption, inelastic scattering, self-scattering of the atoms etc. The forms of these corrections depend on experimental conditions. It has been shown that carefully applied corrections do not alter the structural results and that good agreement can be obtained even if different techniques in various laboratories are applied (see e.g. [48]).

The property which is derived from the diffraction experiments is the structure function

$$k H_\alpha(k) = k(I_{\alpha,\,\mathrm{norm}} - I_{\alpha,\,\mathrm{self}}) \cdot M(k)\,, \tag{2}$$

where α refers to the XD, ND, or ED experiment, $I_{\alpha,\,\mathrm{norm}}$ is the corrected and normalized coherent experimental intensity and $I_{\alpha,\,\mathrm{self}}$ describes the self-scattering of the scattering units; k is the scattering variable, $k = (4\pi/\lambda)\sin\theta$, 2θ being the scattering angle and λ the wavelength of the incident radiation. $M(k)$ is a modification function, used as a k-dependent weight for the structure function. It makes the shape of the $kH(k)$ function more balanced and the structural features better visible. The form of $M(k)$ is arbitrary, and various forms were indeed used for the evaluation of the experimental data discussed here. In order to render the structure functions comparable we convert all functions to a common form with

$$M(k) = \frac{\exp(-bk^2)}{\left(\sum_i x_i\, f_i(k)\right)^2}\,. \tag{3}$$

Here x_i is the atomic fraction of the i^{th} type scattering unit in the molecule and $f_i(k)$ denotes its scattering factor; f_i is k-dependent for the XD and ED experiments, but constant for ND. The value b in the above equation is again an artificial damping factor causing an effect similar to a temperature increase. Since various b-values were used for the experiments, we convert all functions to a form where $b = 0$.

Differences between experimentally determined structure functions can also arise from the fact that either independent atoms or groups of atoms can be used as scattering units. The introduction of group-sites is quite useful in order to reduce the number of partial pair-distributions to be determined. The CH, CH_3 or OH units are often treated in this way. Nevertheless, a certain degree of arbitrariness remains: The contraction of several atoms into a common unit is said to be reasonable when the internal structure of the group does not have a "significant influence" on the overall scattering pattern. The contribution of H-atoms to the XD pattern is, for instance, very low. The H-atom is thus often assumed to form a single scattering center with its neighboring heavy atom. Sometimes it is also simply neglected.

In the ND experiment the scattering factors of both hydrogen and deuterium atoms are comparable in magnitude to those of C, O or N atoms. However, the group-site approach may also be reasonable for these structure functions, provided that the internal structure of the group does not overlap significantly with the intermolecular structure, or that it can be computed with high accuracy. In keeping with the present MD simulation, where the CH_3 groups are treated as group-sites, all experimental data originally in the atomic representation are converted to a form with group form factors assigned to CH_3. In these cases the normalized intensities are re-calculated from the published structure functions and re-normalized according to the self scattering term which includes the new site-definitions. For the XD experiments, the scattering factor of CH_3 is calculated according to an analytical expression given by Narten [49]. For the ND experiments, the scattering factor of the CD_3 group is computed according to

$$f^2_{\mathrm{CD}_3}(k) = f_\mathrm{C}^2 + 9 f_\mathrm{D}^2 + 6 f_\mathrm{D} f_\mathrm{C} \frac{\sin(k r_\mathrm{DC})}{k r_\mathrm{DC}} \cdot \exp\left(\frac{l_\mathrm{DC}^2}{2} k^2\right) \tag{4}$$

where $r_\mathrm{DC} = 1.04$ Å and $l_\mathrm{DC} = 0.02$ Å are typical distances and root-mean-square amplitudes as reported from ND studies on molecules containing CD_3. Careful studies, details of which are not reported here, show that small variations in the above parameters as well as the neglect or inclusion of an additional term for DD interaction do not influence the shape of the overall scattering pattern to an observable extent.

It is interesting to note that by using (4) the ND scattering factor becomes also k-dependent. In the case of H-atoms this treatment would cause significant problems since the scattering factor $f_\mathrm{H} = -3.74$ will make the denominator of (3) very small or even equal to zero. Therefore, the formula for $M(k)$ cannot be used and the application of (4) can be far from accurate. Since ND experiments with several isotopic compositions are available, we avoid the problem of divergence by using experiments with fully deuterated samples only.

Some of the experimental data were reported in a 5-site representation rather than in a 6-site one with contraction of the scattering of the C and H atoms into one group. In the XD cases, the $f_\mathrm{CH}(k)$-form factor calculated by Narten has been used again. For the ND scattering a form factor

$$f^2_\mathrm{CD}(k) = f_\mathrm{C}^2 + f_\mathrm{D}^2 + 2 f_\mathrm{D} f_\mathrm{C} \frac{\sin(k r_\mathrm{DC})}{k r_\mathrm{DC}} \cdot \exp\left(\frac{l_\mathrm{DC}^2}{2} k^2\right) \tag{5}$$

can be used with similar arguments as for CD_3 in (4).

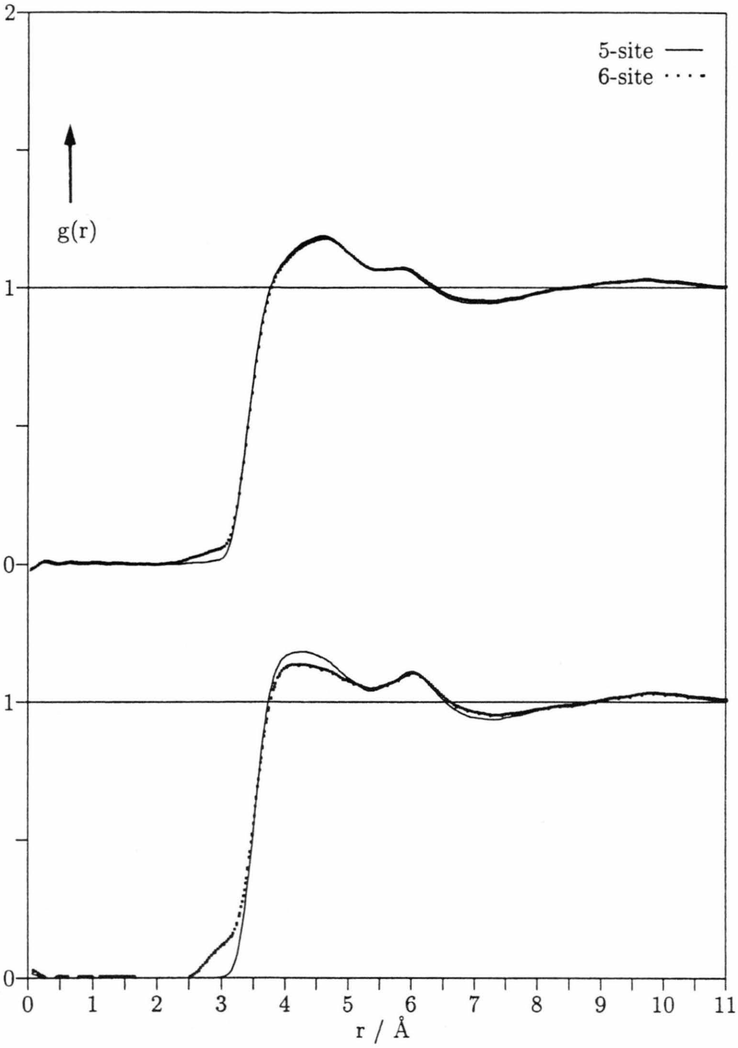

Fig. 1. Pair-distribution functions for liquid DMF from the MD simulations: XD (upper curves) and ND (lower curves) in a 5 and a 6 site representation of the molecule.

In order to show that the total structure function, and consequently the radial distribution function (see below), are not very sensitive to the change from a 6-site to a 5-site representation we calculate the XD and ND structure functions for DMF, starting from the present simulation data, for both cases. The resulting distinct pair-distribution functions are shown in Figure 1.

The change of representation causes almost no effect on the XD radial distributions, while the 5-site representation enhances the main peak and suppresses the small contribution at about 3 Å in the ND. We thus use the 6-site representation in all further cases, except that the 5-site representation was kept for the experimental functions of NMF, where the conversion procedures seem to introduce at least comparable additional errors.

The pair-distribution functions (pdf) are calculated from the structure functions by Fourier transform according to

$$g_\alpha = 1 + \frac{1}{2\pi^2\,\varrho_0\,r} \int k H_\alpha(k)\,\sin(kr)\,\mathrm{d}r\,, \tag{6}$$

where ϱ_0 is the average number density of sites in the liquid. The total structure functions can be separated into intra- and intermolecular parts or, in other terms, "molecular" and "distinct" parts:

$$k H_\alpha(k) = k H_{\alpha,\mathrm{m}}(k) + k H_{\alpha,\mathrm{d}}(k)\,, \tag{7}$$

where the molecular contribution can be calculated by using a suitable geometrical model. The distinct term is then given by subtraction of the molecular term from the total structure function. The corresponding "distinct" term for the pair-distribution function is calculated again by Fourier transform:

$$g_{\alpha,\mathrm{d}}(r) = 1 + \frac{1}{2\pi^2 \varrho_0 r} \int k\left(H_\alpha(k) - H_{\alpha,\mathrm{m}}(k)\right) \sin(kr)\, \mathrm{d}r\,. \tag{8}$$

IV. Results and Discussion of the Structures

Experimental distinct structure functions are compared with the ones calculated from the present MD simulation in Figs. 2 and 3 and the corresponding pair-distribution functions are shown in Figures 4 and 5. For the sake of clarity, only one experimental function is presented for each liquid. The one with the most detailed analysis of the intermolecular structure is selected for this purpose. The experimental data not shown are in a similar agreement with the MD as those presented here. Figure 6 shows that the agreement between two independent XD measurements of the total pair-distribution functions of liquid DMF [9–10] is indeed very good. The only visible difference is in the amplitude of the first peak, assigned to the shortest intramolecular distances, and it may be considered insignificant.

A) Formamide

The 6-site representation, which is the atomic site-representation for formamide, is used in all studies. Therefore, no site-conversion is needed. The distinct XD structure functions are calculated from the total structure functions published by Ohtaki et al. [1]. The molecular contribution is calculated with the inclusion of the C=O, C–N and N ··· O terms only, and by using the structural parameters ($r_{\mathrm{CO}} = 1.24$ Å, $r_{\mathrm{CN}} = 1.33$ Å, $r_{\mathrm{NO}} = 2.25$ Å, $l_{\mathrm{CO}} = 0.058$ Å, $l_{\mathrm{CN}} = 0.06$ Å, and $l_{\mathrm{NO}} = 0.075$ Å) reported there. Since the H-atom positions were not determined, they are neglected. This approximation can, however, cause inaccuracies since the contribution of all pairs involving an H-atom can reach 20–25% of that of the heavy atoms. The ND distinct structure function was published separately for liquid FA [2, 3]; only an appropriate rescaling of the data is necessary here.

From Figs. 2 and 3 it seems that the agreement between experiment and simulation is much better for the ND data than for XD. The shape and depth of the first minimum is, however, well reproduced by the simulation both for XD and ND, which suggests that the intermediate and long range structures are in good agreement. This is also seen in the corresponding pair-distribution functions (Figs. 4 and 5) for separations around 5 Å and above. The main maximum of the $kH(k)$ functions is reproduced in shape (peak followed by a shoulder and minimum) in both cases, but the positions are in better agreement with experiment for XD than for ND. The minor peaks show the correct amplitudes for ND and are overestimated for XD, where some of them are shifted. This mixed behavior of partial agreement and disagreement can be better understood with the help of the corresponding pair-distribution functions.

The experimental XD-weighted g-function has 3 main peaks at about 3 Å, 3.8 Å, and 4.8 Å, while the MD curve gives only a small contribution around 3 Å. An enhanced main peak emerges at about 3.6 Å, followed by the shoulder-peak shifted down to about 4.3 Å. The main peak is seemingly the superposition of the first two experimental peaks. The same feature is seen, but to a lesser extent, for the ND pair-distribution functions. Here it is interesting to observe that the peak at 2 Å is higher for the experimental function than for the simulated one.

The assignment of the peaks in the experimental total g-functions can be done easily from the simulation data. In a 6-site representation there are 21 different pdf's. The positions of characteristic points of a number of them are intercompared with ones obtained from other MC [4] and MD [5] simulations in Table 5.

Based on the pair-distribution functions from the present simulation, a model can be constructed for the average local arrangement of FA molecules. In the FA molecule the center of mass practically coincides with

Table 5. Comparison of the characteristic data of several partial pair-distribution functions for liquid FA.

	This work		MC-Simulation [4]		MD-Simulation [5]	
	first max. $r/\mathrm{Å}$	first min. $r/\mathrm{Å}$	first max. $r/\mathrm{Å}$	first min. $r/\mathrm{Å}$	first max. $r/\mathrm{Å}$	first min. $r/\mathrm{Å}$
O···N	347	520	290	369	310	454
O···H1(N)	277	493	197	282	216	295
O···H2(N)	277	493	197	282	223	295
O···H(C)	277	410	–	–	–	–
N···N	373, 493	603	380	595	353, 490	590
C···N	393	580	378	611	378	583
C···C	433	610	418, 444	576	418	576

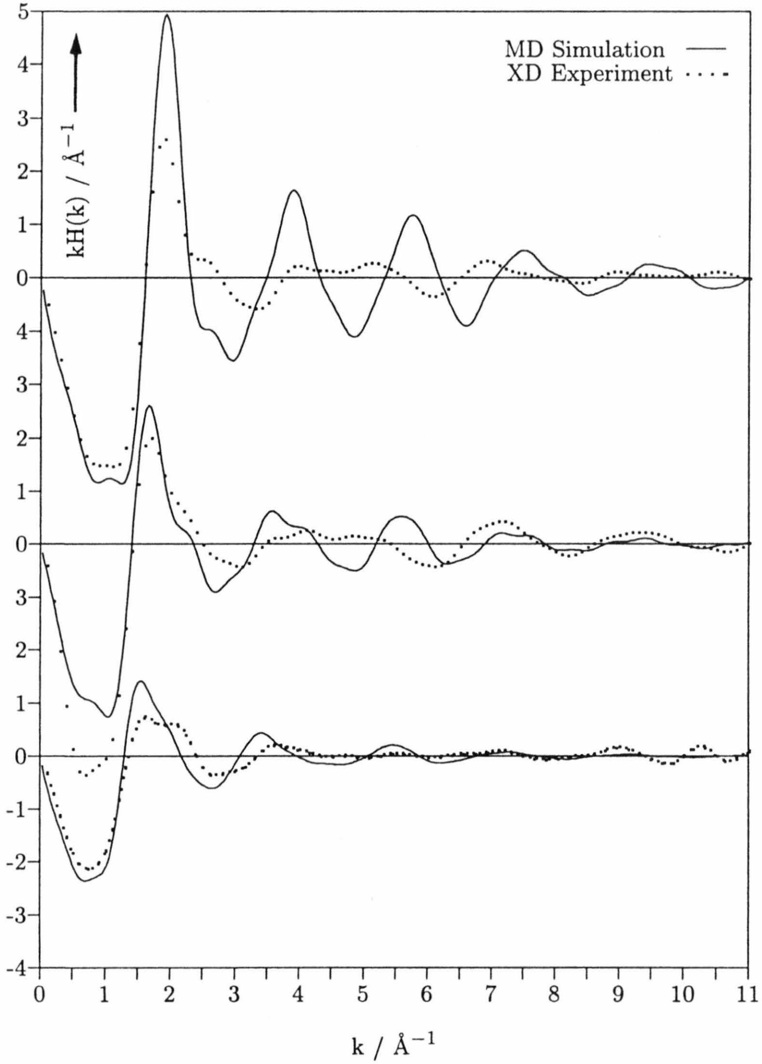

Fig. 2. Distinct structure function for liquid FA (top), NMF (middle) and DMF (bottom) derived from XD experiments and their calculated equivalents from the MD simulation.

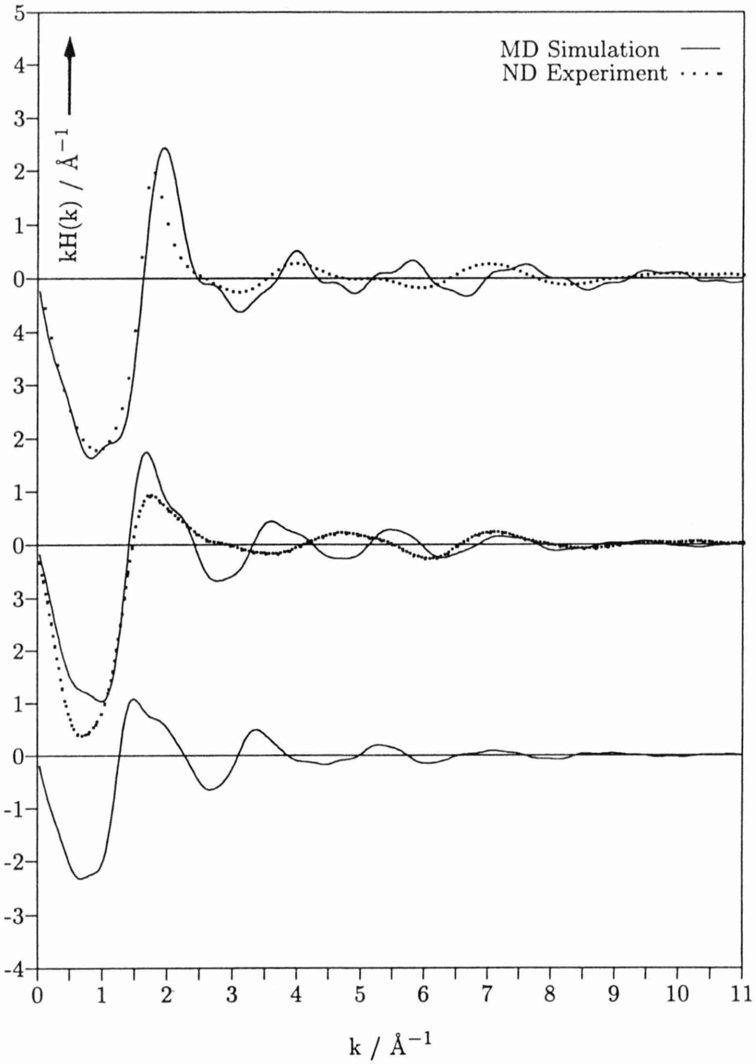

Fig. 3. Distinct structure function for liquid FA (top), NMF (middle) and DMF (bottom) derived from ND experiments and their calculated equivalents from the MD simulation.

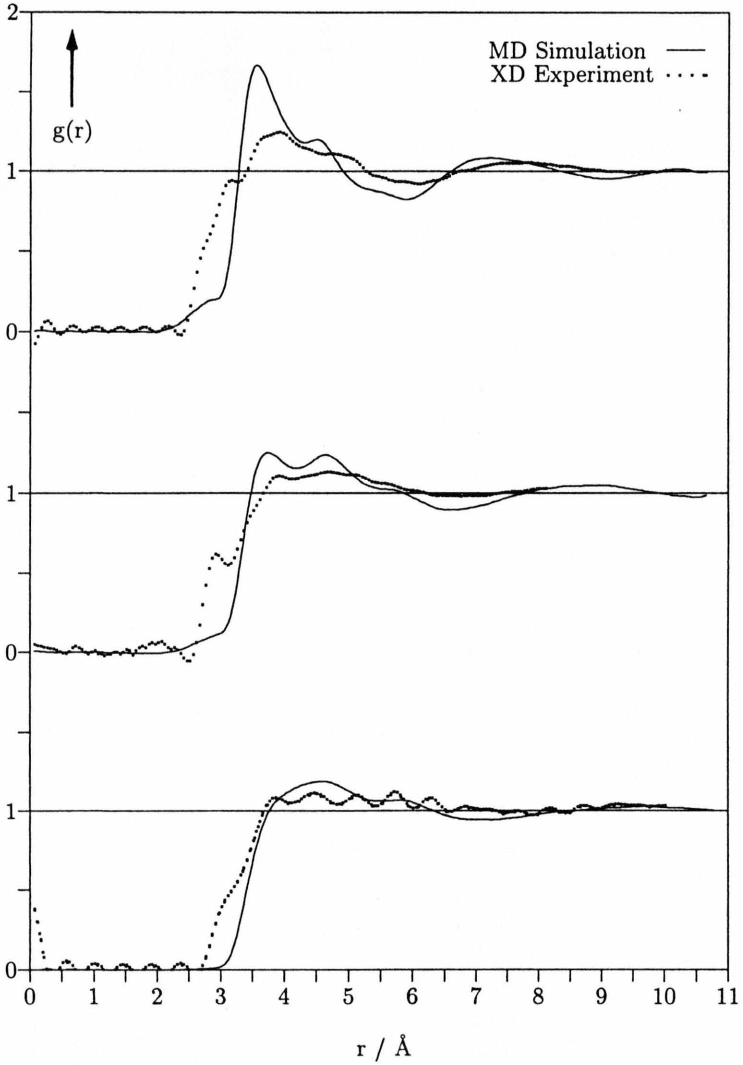

Fig. 4. Distinct pair-distribution function for liquid FA (top), NMF (middle) and DMF (bottom) derived from XD experiments and their calculated equivalents from the MD simulation.

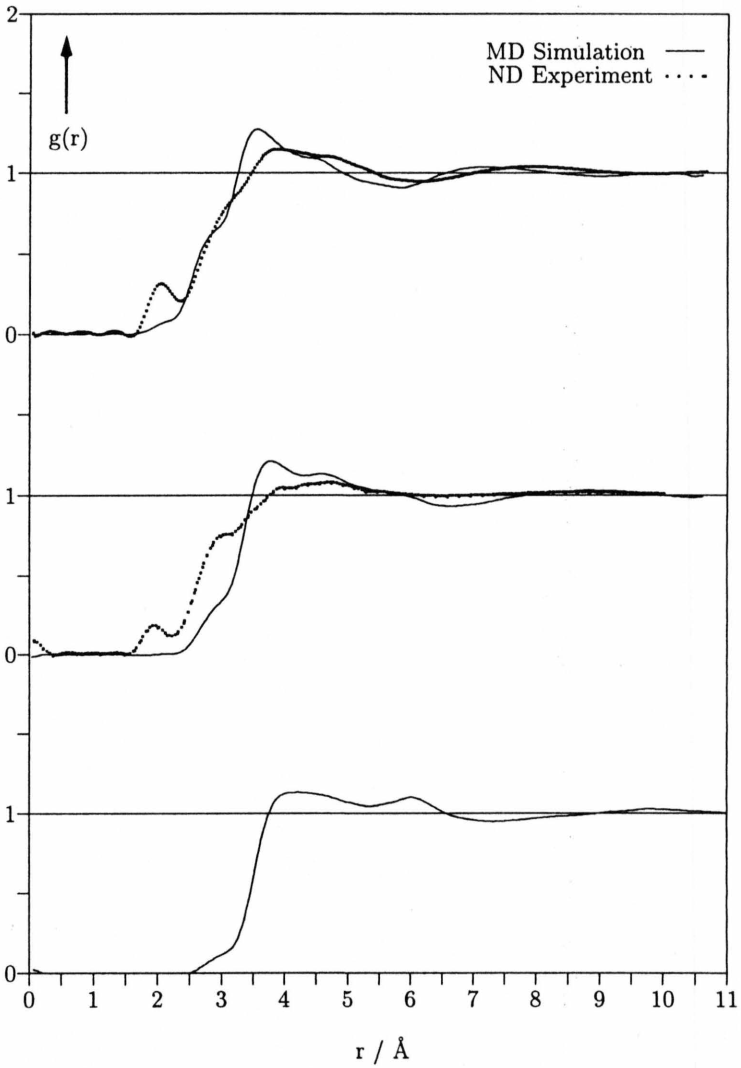

Fig. 5. Distinct pair-distribution function for liquid FA (top), NMF (middle) and DMF (bottom) derived from ND experiments and their calculated equivalents from the MD simulation.

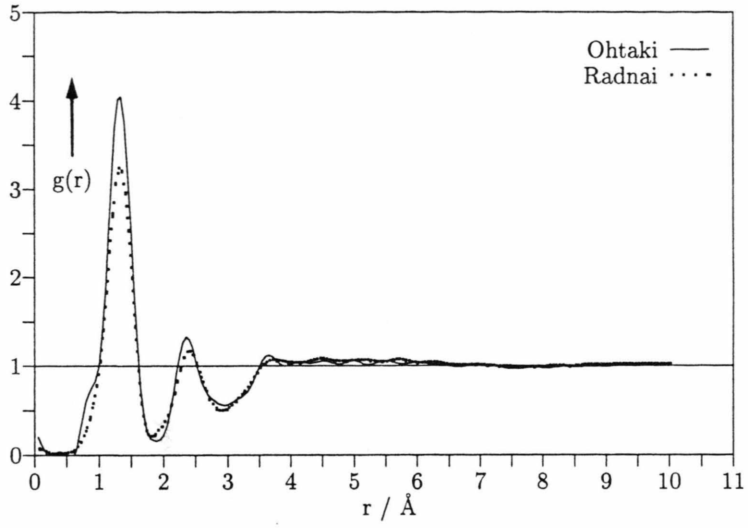

Fig. 6. Total pair-distribution functions of liquid DMF obtained from two independent XD experiments [9, 10].

the position of the C-atom. Therefore, the distribution of the C–C distances measures roughly the distribution of molecular centers. The simulated average center-center distance between two adjacent molecules is about 4.33 Å. Comparing our results with the values obtained from the previous simulations [4, 5], the C–C distance and also the position of the first minimum at 6.1 Å are in excellent agreement, the corresponding distances being 4.27 Å and 5.97 Å. The ND experiment also yields a C–C distance of 4.2 Å. The integration of the simulated C–C pdf up to the first maximum and minimum results in coordination numbers of 4 and 13.8, also in good agreement with previous MD results (4 and 12.82).

The value of 13.8 is also in agreement with the sum of the coordination numbers obtained for the O–H(N) partial pdf's first minimum, namely $6.8 + 6.7 = 13.5$. These data show that the location of the nearest neighbor molecules as well as the extension of the first coordination shell are described by all models in a similar way. Since the distinct pdf's are composed of all partial pdf's, it is difficult to locate most of the distances in the experimental (and calculated) functions in Figs. 2 and 3.

We consider now the hydrogen-bonding in liquid FA. The integration of the O–N partial pdf up to its first minimum at 5.2 Å yields about 4.5. This is somewhat higher than 4, the largest possible number of ideal hydrogen bonds per molecule. This value was reported for all experiments and simulations; it means that all hydrogens are thought to participate in H-bonds in the liquid. The present value is not in contradiction to these results. This is seen by considering that the first maximum of the O–N pdf is highly asymmetric and the integration thus certainly includes a number of atoms located beyond the H-bonds.

However, the average length of the hydrogen bonds is larger here than reported previously. This is seen both from the O–H and the O–N distributions in Table 5. This result is rather surprising if we consider that the average separation of the molecular centers and the average number of H-bonds is in agreement with the accepted values. While the elongation of these bonds is certainly not realistic, the examination of the reasons can help to understand some characteristics of the structure of FA and of molecular liquids in general.

At a fixed center-center distance of about 4.3 Å an elongated hydrogen bond can be created only by pairs of molecules with angles between their planes significantly different from zero. For cyclic dimers both molecules must lay in the same plane. For a chain structure slight variations in the orientations can occur. This is possibly more favorable in the liquid state and may be the reason why the lower energy dimer (see below) is less frequent there.

Previous studies were somewhat contradictory with respect to the predominant form of molecular dimers in the liquid (or, in other words, the mutual orientation of the nearest neighbors). A consensus seemed later to arise from the diffraction studies, claiming a predominant chain structure rather than ring dimers. MC and MD simulations emphasize the same result with a slight doubt, however, since ab initio calculations [5] lead to lower energies for ring dimers than for linear dimers. The present simulation, in fact, reveals a mixture of ring and chain conformations with neighbors oriented with their molecular axes and dipole moments both parallel and perpendicular. We also remark that all 6 dimer forms suggested by Sagarik et al. [5] are found in the simulation.

It has often been questioned to which extent differences in the potentials can influence the intermolecular structure functions and pair-distribution functions in the case of dipolar linear molecules [51]. However, it can not be excluded that the attractive part of the intermolecular O–H model potential is too shallow. This would be in contrast to the findings for other hydrogen bonded liquids modelled in the same way, but a potential where the sigma value for the H-atom was completely removed has been used in a MC simulation [4]. Moreover in a recent ND study on solid FA at 7 K [50] the authors had to substitute the exp-6 of the repulsive term of the O–H potential term by an exponential attraction cut-off at 3 Å in order to localize the H-atoms in the crystal. The Lennard-Jones type potential plus partial charges is thus certainly not always an efficient way to reproduce the main features of the hydrogen bonded liquids.

B) N-Methylformamide

An XD experiment has been reported for liquid *N*-methylformamide by Ohtaki et al. [6]. Unfortunately, the data for the structure functions are no longer available in their original form. Instead, we use the unpublished XD and ND data by Pálinkás et al. [8]. Both data sets are in a 5-site form. The comparison of the structure and pair-distribution functions reveals a much better agreement between the experimental and the MD curves than for FA. The heights of the main and the smaller peaks of the structure function agree quite well, with the exception of the broad peak at 4 Å^{-1} in the ND structure function which bridges the two peaks of the curve obtained by the MD calculation. The distinct pair-distribution functions show an acceptable agreement above 3–3.5 Å, although the MD simulation seems to overestimate the ordering in this region. The peaks (or rather shoulders) appearing at 2 Å and 3 Å in the XD and ND experimental functions are not well reproduced by the MD simulation, similarly to what was found for the formamide. The explanation is probably the same: the O···H and O···N hydrogen-bond distances are longer in the simulated liquids, but the other heavy atom positions as well as the distribution of the center-center distances exhibit good agreement.

Table 6. Comparison of the characteristic data of several partial pair-distribution functions for liquid NMF.

	This work		MC-Simulation [8]	
	first max. $r/\text{Å}$	first min. $r/\text{Å}$	first max. $r/\text{Å}$	first min. $r/\text{Å}$
O···N	360	560	283	348
O···Me	360	530	362	525
O···H(N)	270	407	186	283
O···H(C)	286	393	–	–
N···N	483	683	497	683
C···N	460	680	390, 506	650
C···C	460	683	456	688

Numerical data representing the pair-distribution functions are listed in Table 6. The center of mass of the NMF molecule is located between the C and N atom, both C–C and N–N pdf's have their first maximum and minimum at about the same distance. Accordingly, the average separation distance between two adjacent molecules is about 4.6 Å, roughly 0.3 Å more than for FA. The first coordination shell extends to about 6.8 Å, where the first minima are located. The larger intermolecular separation is in keeping with the increased volume of the molecule due to the bulky methyl group. The integration of the pdf's gives 3 neighbors until the first maximum and 13 until the minimum, a slightly smaller value than for the FA. The hydrogen bonds are again elongated. A recent MC simulation [8] without LJ-center on the hydrogen and with a reduced σ_{OO} of 2.96 Å (instead of 3.405 Å used here, see Table 3) yields hydrogen bond lengths closer to the experimental values. The partial charges used in the model potentials are also somewhat different (O: −0.500 (OPLS), −0.479 (this work); H: 0.425 (OPLS), 0.300 (this work)). Due to the 6-site representation, the distinction between the two possible conformations (cis- and trans-) of the NMF molecules cannot be made from the present simulation. The present somewhat controversial state was discussed by Neuefeind et al. [7].

C) N,N-Dimethylformamide

Two XD experiments are available for liquid DMF, they are in good agreement with each other, see Figure 6. The distinct XD structure function is derived from the observed total structure function by subtracting a molecular contribution from geometrical model parameters given by Radnai et al. [10]. It is worth noting here that recently an electron diffraction study of the structure of the DMF molecule in the gas phase [52] has led to a somewhat different set of parameters. According to this report the two methyl groups are nearer to each other than it was found from the XD data in the liquid phase and from other previous studies (2.42 Å instead of 2.61 Å). This discrepancy in the molecular geometry can be due to difficulties in interpreting the data for the liquid phase, but a small change in the average structure when going from the gas to the liquid phase can not be excluded. Since ND investigations have not been performed on liquid DMF, a further check of the intramolecular structure in liquid is indeed needed.

The comparison of the XD structure functions from the experiment and from the MD simulation shows the best agreement among the three amides studied. Although the experimental structure function gives a lower and broader main peak with a double maximum instead of the higher peak on the MD curve, the overall shapes of the distinct functions are close to each other. The bulk of the pair-distribution functions is also reproduced rather well: The spurious peaks on the experimental curve cover a broad and flat maximum and minimum, while the MD curve exhibits again a somewhat stronger structural feature. The ND structure and pair-distribution functions are predicted from the MD simulation. The structure function shows a flatter main peak with a shoulder, similar to the XD experimental function. On the other hand, the ND pdf becomes more structured, especially in the range around 6 Å. Even if the degree of local order as seen from the distinct curves is somewhat exaggerated, it suggests that the liquid DMF is not at all "structureless" as it has been often supposed. Relatively strong correlation seems to exist between neighboring molecules. The characteristic features of the partial pdf's (Table 7) are in keeping with those for FA and NMF.

Table 7. Comparison of the characteristic data of several partial pair-distribution functions for liquid DMF.

	This work		MC-Simulation [4]		MD-Simulation [11]	
	first max. $r/\text{Å}$	first min. $r/\text{Å}$	first max. $r/\text{Å}$	first min. $r/\text{Å}$	first max. $r/\text{Å}$	first min. $r/\text{Å}$
O···N	440	614	446	600	446	600
O···Me1	367	503	368	451	376	488
O···Me2	367	553	368	557	376	557
O···H	287	453	–	–	–	–
N···N	550	743	550	750	560	750
C···N	500	750	500	770	500	770
C···C	447	510	440	510	–	–

The center-center correlation is approximately measured by the N–N distribution. The separation distance corresponding to the first maximum in the N–N pdf is shifted further to 5.5 Å, where the integration yields 4.2 neighbors. The position of the minimum is at 7.43 Å, with the same coordination number of 13 as for NMF. These values agree well with those from MC and other MD simulations, so do the distinct $g(r)$-functions. We call Me1 the methyl group next to the oxygen atom. It is interesting to observe that the O–Me1 pdf shows a second small maximum at 5.9 Å with a height of 1.08 while the O–Me2 function does not. The first peak of the O–Me2 pdf is higher than the corresponding one of the O–Me1 pdf. If two molecules are roughly parallel to each other, the Me2-group of one molecule is "fixed" by the O-atom of the other molecule at a distance of 3.7 Å. This also fixes the O–Me1 distance at 5.9 Å. Only the strong O–Me2 correlation is able to induce this additional O–Me1 correlation. A stronger correlation of the O-atom with the Me2-group was also found by NMR spectroscopic studies where the Me1 groups are seen to rotate much faster than the Me2 ones in liquid DMF [53].

An approximate geometrical model constructed to describe the local order in liquid DMF [10] has been used to interpret the XD experimental structure functions under the assumption that two adjacent molecules are oriented predominantly in an antiparallel way. The present simulation reproduces this result quite well, the angle between the dipoles of neighboring molecules being close to 180 degrees. A small number of perpendicularly aligned molecule-pairs is, however, also found.

V. Conclusions

In the present work we attempt to compare in an unbiased way the direct structural information available for liquid amides at room temperature from a number of experimental sources with existing and new simulation results. For this purpose consistent model potentials are developed for molecular dynamics simulations of formamide, N-methylformamide and N,N-dimethylformamide. The comparison is carried out for the X-ray and neutron weighted structure functions and radial pair-distribution functions.

For the three liquids there is reasonable agreement between the various approaches as far as the distribution of the intermolecular distances between heavy atoms are concerned, although typically the simulations have a tendency to overestimate the structure. The main disagreement concerns the length of the hydrogen bonds in the liquid, a quantity which is difficult to determine experimentally. It seems, however, that the models used consistently lead to an overestimation of the length of these bonds.

Two models have been mainly used in the literature to interpret the structure of these liquids, which can be roughly summarized under the headings "linear dimers" or "cyclic dimers". Since the simulations give access to all radial pair-distribution functions, they allow not only comparisons with experimental results but also consistency checks of these functions with the various proposed interpretations. The direct detection and visualization of local structures is also possible. From such an analysis, the present simulations yield a mixture of linear and cyclic conformations with a significant amount of T-shape configurations for FA. The same is found for NMF, while a predominant antiparallel orientation of neighboring molecules is postulated for DMF.

Acknowledgement

A grant of computer time on the "Landesvektorrechner NRW (SNI S600/20)" at the computer center of the RWTH is gratefully acknowledged. P. B. also acknowledges the award of a Heisenberg Fellowship from DFG, and support by Fonds der Chemischen Industrie, Frankfurt, is also acknowledged. T. R. is grateful to the Deutsche Forschungsgemeinschaft and to the Hungarian National Scientific Research Fund (OTKA), project number 1087 (459/91), for partial financing of this project. Thanks are due to H. Ohtaki, S. Itoh, and F.-J. Wiesmann for experimental data, and to G. Pálinkás who made his data available to us prior to publication.

[1] H. Ohtaki, A. Funaki, B. M. Rode, and G. J. Reibnegger, Bull. Chem. Soc. Japan **56,** 2116 (1983).

[2] E. Kálmán, I. Serke, G. Pálinkás, M. D. Zeidler, F.-J. Wiesmann, H. Bertagnolli, and P. Chieux, Z. Naturforsch. **38a,** 231 (1983).

[3] F.-J. Wiesmann, M. D. Zeidler, H. Bertagnolli, and P. Chieux, Mol. Phys. **57,** 275 (1986).

[4] W. L. Jorgensen and C. J. Swenson, J. Amer. Chem. Soc. **107,** 569 (1985).

[5] P. K. Sagarik and R. Ahlrichs, J. Chem. Phys. **86,** 5117 (1987).

[6] H. Ohtaki, S. Itoh, and B. M. Rode, Bull. Chem. Soc. Japan **59,** 271 (1986).

[7] J. Neuefeind, P. Chieux, and M. D. Zeidler, Mol. Phys. **76,** 143 (1992).

[8] G. Pálinkás et al. to be published.

[9] H. Ohtaki, S. Itoh, T. Yamaguchi, S. Ishiguro, and B. M. Rode, Bull. Chem. Soc. Japan **56,** 3406 (1983).

[10] T. Radnai, S. Itoh, and H. Ohtaki, Bull. Chem. Soc. Japan **61,** 3845 (1988).

[11] S. Yasbonath and C. N. R. Rao, Chem. Phys. **155,** 351 (1991).

[12] G. Fogarasi, P. Pulay, F. Török, and J. E. Boggs, J. Mol. Struc. **57,** 259 (1979).

[13] D. H. Christensen, R. N. Kortzeborn, B. Bak, and J. J. Led, J. Chem. Phys. **53,** 3912 (1970).

[14] C. W. Bock, M. Trachtman, and P. George, J. Amer. Chem. Soc. **101,** 5122 (1979).

[15] M. Kitano and K. Kuchitsu, Bull. Chem. Soc. Japan **47,** 631 (1974).

[16] R. J. Kurland and E. B. Wilson, Jr., J. Chem. Phys. **27,** 585 (1957).

[17] E. D. Stevens, Acta Cryst. **B 34,** 544 (1978).

[18] E. Hirota, R. Sugisaki, C. J. Nielsen, and G. O. Sorensen, J. Mol. Spectrosc. **49,** 251 (1974).

[19] M. Kitano and K. Kuchitsu, Bull. Chem. Soc. Japan **47,** 67 (1974).

[20] L. V. Vilkov, P. A. Akishin, and V. M. Presnyakova, J. Struct. Chem. **3,** 3 (1962).

[21] A. Annamalai and S. Singh, J. Chem. Phys. **77,** 860 (1982).

[22] J. F. Yan, F. A. Momany, R. Hoffmann, and H. A. Scheraga, J. Phys. Chem. **74,** 420 (1970).

[23] M. Rigby, E. B. Smith, W. A. Wakeham, and G. C. Maitland, The Forces Between Molecules, Clarendon Press, Oxford 1986.

[24] H. J. Böhm, I. R. McDonald, and P. A. Madden, Mol. Phys. **49,** 347 (1983).

[25] P. A. Bopp, in: Software-Entwicklung in der Chemie (J. Gasteiger, Hrsg.), Springer-Verlag, Berlin 1987.

[26] H. Guo and M. Karplus, J. Phys. Chem. **96,** 7273 (1992).

[27] W. L. Jorgensen and J. M. Briggs, Mole. Phys. **63,** 547 (1988).

[28] W. Dietz and K. Heinzinger, Ber. Bunsenges. Phys. Chem. **88,** 543 (1984).

[29] C. S. Muethy, K. Singer, M. L. Klein, and I. R. McDonald, Mole. Phys. **41,** 1387 (1980).

[30] C. L. Kong, J. Chem. Phys. **59,** 2464 (1973).

[31] Y. Sugawara, Y. Hamada, A. Y. Hirakawa, M. Tsuboi, S. Kato, and K. Morokuma, Chem. Phys. **50,** 105 (1980).

[32] Y. Sugawara, Y. Hamada, M. Tsuboi, S. Kato, and K. Morokuma, Chem. Phys. **62,** 339 (1981).

[33] G. Durgaprasad, D. N. Sathyanarayana, and C. C. Patel, Bull. Chem. Soc. Japan **44,** 316 (1971).

[34] G. Fogarasi and A. Balazs, J. Mol. Struct. (Theochem) **133,** 105 (1985).

[35] V. V. Chalaphathi and K. V. Ramiah, Prod. Ind. Acad. Sci. **68,** 109 (1968).

[36] E. D. Schmid and E. Bordbek, J. Chem. Phys. **78,** 1117 (1983).
[37] E. D. Schmid and E. Brodbek, J. Mol. Struct. **108,** 17 (1984).
[38] G. Kaufmann and M. J. F. Leroy, Bull. Soc. Chim. Fr. **2,** 402 (1967).
[39] K. Itoh and Shimanouchi, J. Mol. Spectrosc. **63,** 306 (1981).
[40] Y. Tanaka and K. Machida, J. Mol. Spectrosc. **63,** 306 (1976).
[41] A. Balazs, Acta Chim. Acad. Sci. Hung. **108,** 265 (1981).
[42] R. L. Jones, J. Mol. Spectrosc. **11,** 411 (1963).
[43] T. C. Jao, I. Scott, and D. Steele, J. Mol. Spectrosc. **92,** 1 (1982).
[44] S. Ataka, H. Takeuchi, and M. Tasumi, J. Mol. Struct. **113,** 147 (1984).
[45] D. E. DeGraaf and G. B. B. M. Sutherland, J. Chem. Phys. **26,** 716 (1956).
[46] P. P. Ewald, Ann. Phys. **64,** 253 (1921).
[47] M. P. Allen and D. J. Tildesley, Computer Simulation of Liquids, Clarendon Press, Oxford 1987.
[48] M. Magini, G. Licheri, G. Paschina, G. Piccaluga, and G. Pinna, X-Ray Diffraction of Ions in Aqueous Solutions: Hydration and Complex Formation, CRC Press, Boca Raton, FL 1988.
[49] A. H. Narten, J. Chem. Phys. **70,** 299 (1979).
[50] B. H. Torrie, C. O'Donovan, and B. M. Powell, Mol. Phys. **82,** 643 (1994).
[51] T. Radnai and P. Jedlovszky, J. Phys. Chem. **98,** 5994 (1994), and references therein.
[52] G. Schultz and I. Hargittai, J. Phys. Chem. **97,** 4966 (1993).
[53] R. Konrat and H. Sterk, J. Phys. Chem. **94,** 1291 (1990).